



OPEN

SUBJECT AREAS:

PERMEATION AND
TRANSPORT

ION TRANSPORT

Received

2 August 2013

Accepted

16 December 2013

Published

10 January 2014

Correspondence and
requests for materials
should be addressed to
S.O. (oiki-fki@umin.ac.
jp)

Paradoxical One-ion Pore Behavior of the Long β -Helical Peptide of Marine Cytotoxic Polytheonamide B

Masayuki Iwamoto¹, Shigeki Matsunaga² & Shigetoshi Oiki¹¹Department of Molecular Physiology and Biophysics, Faculty of Medical Sciences, University of Fukui, Fukui 910-1193, Japan,²Laboratory of Aquatic Natural Products Chemistry, Graduate School of Agricultural and Life Sciences, The University of Tokyo, Bunkyo-ku, Tokyo, 113-8657, Japan.

The cytotoxic 48-mer peptide, polytheonamide B (pTB), from a marine sponge forms a $\beta^{6.3}$ -helix with an inner diameter of 4 Å and a length of 45 Å, features that allow the selective permeation of monovalent cations across targeted cell membranes. To characterize this long, narrow pore, electrophysiological examination using a planar lipid bilayer method was performed. The single-channel current amplitude exhibited saturation for concentrated Cs⁺ or K⁺ solution, and the reversal potential in mixed solutions did not exhibit any anomalous mole-fraction behavior. These results suggest the one-ion permeation mechanism. This is in contrast to the short (26 Å) $\beta^{6.3}$ -helical gramicidin channel, which holds two ions simultaneously. The paradoxical one-ion permeation through the long pTB channel was modeled with a discrete-state Markov model. Ions permeate through the channel by stepping between two binding sites in the pore, but never occupy these sites simultaneously in either pure or mixed ion solution.

Polytheonamide B (pTB) is a potent cytotoxic peptide obtained from the marine sponge *Theonella swinhoei*, and its cytotoxicity is especially high in mammalian cells, even at concentrations as low as ng/ml^{1–3}. The pTB 48-mer peptide possesses certain unique structural features, such as D- and L-amino acid side chains taking alternate positions throughout the sequence, and also the presence of many unusual amino acids (Fig. 1 legend)^{4–7}. Structural studies in an organic solvent revealed that pTB forms a right-handed $\beta^{6.3}$ -helix having a pore of 4 Å in diameter (Fig. 1)⁸, similar to a previously well-characterized antibiotic, gramicidin A (gA)⁹.

We have demonstrated that pTB exhibits ion channel activity at below pico molar concentrations through vectorial insertion into the membrane^{1,3}. Once incorporated, pTB stays there and never escapes from the membrane. These features of pTB constitute the origin basis of its potent cytotoxicity¹⁰. For the permeation properties, we have examined the single-channel current of the pTB channel in the planar lipid bilayer, including single-channel conductance and selectivity among monovalent cations. The selectivity sequence of the alkali cations (Cs⁺ > Rb⁺ > K⁺ > Na⁺ > Li⁺) of the pTB channel is shared with the gA channel, and is characteristic of the $\beta^{6.3}$ -helical narrow pore rendering a single-file permeation¹¹.

Alternate L- and D-chirals of pTB in the amino acid sequence, shared with the gA channel, is prerequisite to make the helix inside hollow for ion permeation, but never observed in proteins. This backbone structure is configured for the carbonyl oxygens to interact with permeating ions. In this respect, the potassium channel proteins has the selectivity filter, which takes unusual configuration of the peptide backbone with participation of achiral glycine residues^{12–14}, and rendering the backbone carbonyls solvating the permeating ions. Thus, in both pTB and KcsA cases, including gA, the backbone configuration is arranged such that the carbonyl oxygens can interact with the permeating ions. Totally different appearance of the pore structure of the pTB channel and the potassium channels may share some permeation properties.

In this study we examined the permeation properties of the pTB channel in more detail with respect to the multi-ion nature of permeation^{15,16}. Compared to the short gA channel (i.e. the head-to-head dimer of the 15-mer peptide) which is 26 Å in length for just spanning the hydrophobic core of the membrane^{11,17}, the pTB channel is 45 Å in length (i.e. a monomer of a 48-mer peptide) and readily forms a long pore in the membrane. It has been established that the short-pore gA channel simultaneously holds two ions during the permeation of Cs⁺, Rb⁺ and K⁺^{18,19}, and one considers that two or more ions could occupy the long pTB channel. Here we applied conventional methods for examining the multi-ion nature of the pTB channel, such as the concentration dependency of the single-channel current amplitude and changes in the reversal potential (V_{rev}) in mixed ion solutions, which is

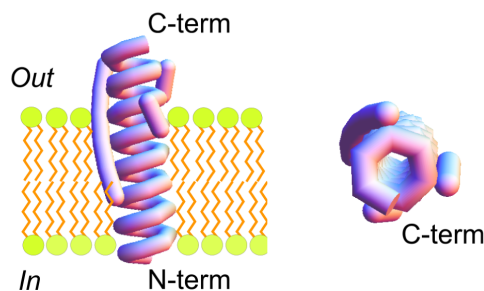


Figure 1 | A schematic representation of the pTB channel embedded in the membrane. The amino acid sequence of pTB is: Gly-L-Mil-Gly-L-Tle-D-Tle-L-Tle-D-Ala-L-Tle-D-Tle-L-Ala-Gly-L-Ala-D-Tle-L-Ala-D-Asm-L-Hva-Gly-L-Ala-Gly-L-Tle-D-Asm-L-Mgn-D-Hva-L-Ala-Gly-Gly-D-Asm-L-Ile-D-Ham-L-Tle-D-Hva-Gly-D-Asm-L-Ile-D-Asm-L-Val-D-Ham-L-Ala-D-Asm-L-Val-D-Ser-L-Val-D-Asn-L-Mme-D-Asn-L-Gln-D-aTh-L-Thr (Mil: β -methylisoleucine, Tle: *tert*-leucine, Asm: γ -N-methylasparagine, Hva: β -hydroxyvaline, Mgn: β -methylglutamine, Ham: γ -N-methyl-*threo*- β -hydroxyasparagine, Mme: β , β -dimethylmethionine sulfoxide, aTh: *allo*-threonine). pTB forms a β -helix with 6.3 residues per turn ($\beta^{6.3}$ -helix), in which an open pore is generated with a uniform inner diameter of 4 Å. The inner surface of the pore is lined with the peptide backbone and allows monovalent cation permeation. The outer surface is covered with hydrophobic residues, and some of them form hydrogen-bonded chains along the longitudinal axis (the long and short strands) and reinforce the helix structure. The 45 Å long channel is inserted into the membrane lead by the N-terminal end and readily spans the membrane.

referred to as the “mole-fraction experiment”^{20–22}. These results indicated that, in contrast to the expectation, the pTB channel allows only one ion at a time to be in the channel upon permeation. The permeation property was further analyzed using the well-established permeation model (the discrete-state Markov model^{23–26}). Underlying mechanism of the paradoxical one-ion pore feature for the pTB channel is discussed in comparison with the gA channel.

Results

The single-channel permeation properties of the pTB channel.

The pTB channel allows permeation of Cs⁺ most efficiently among the monovalent alkali cations¹, so we examined the permeation properties of the pTB channel in CsCl solution. Figure 2A displays the typical single-channel current traces of the pTB channel recorded at various membrane potentials in the 3 M of symmetrical CsCl solution. Frequent transitions between open and closed states were observed at both positive and negative membrane potentials¹. The open dwell time differed substantially at different membrane potentials, indicating that the pTB has weak voltage-dependent gating³. The current-voltage (*i*-*V*) relationships of the single-channel current are depicted in Fig. 2B. The shape of the *i*-*V* curve tended to be supra-linear at high membrane potentials in Cs⁺ concentrations of 1 to 3 M. These results of the single-channel *i*-*V* relationship are qualitatively similar to those for the gA channels at high ion concentrations⁹, suggesting that the rate-determining step for ion permeation is not the entry of the ion into the pore, but rather, the translocation process across it^{19,27}. The *i*-*V* curve exhibited a slight inward-rectification, reflecting the asymmetry of the permeation pathway^{28–30}.

The amplitude of the unitary current of the pTB channel increased substantially with an increasing Cs⁺ concentration (the *i*-*C* curve), exhibiting saturation at all the membrane potentials examined¹ (Fig. 2C). This feature is different from the gA channel, which exhibits a decline of single-channel conductance at high Cs⁺-concentrations¹¹. Similar single-channel measurements and analysis were performed for K⁺ (see Suppl. Fig. S1). The conductance of K⁺ was less than half that of Cs⁺, but the shape of the *i*-*V* and *i*-*C* curves are

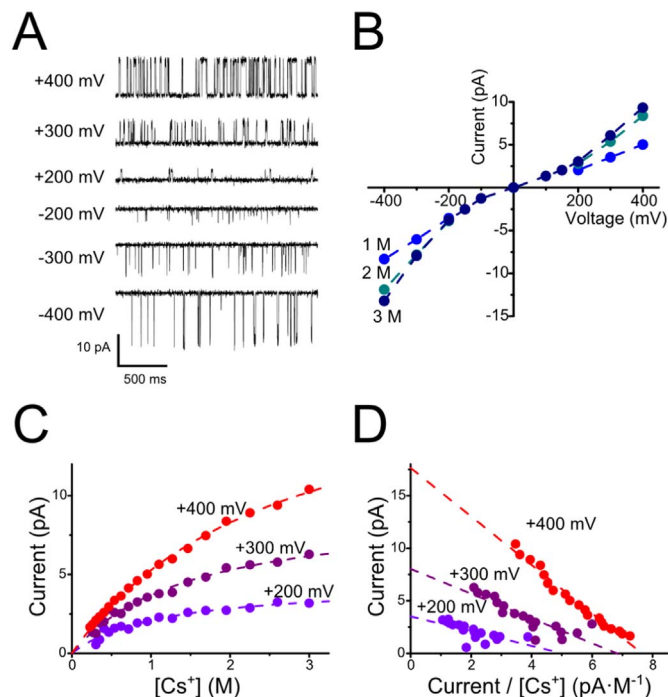


Figure 2 | Properties of single-channel current of the pTB channel for Cs⁺ permeation. (A). The single-channel current of the pTB channel in the symmetric Cs⁺ solution. The Cs⁺ concentration was 3 M. The membrane potential is defined as the *trans* compartment relative to the *cis* compartment, to which pTB was added. The upward deflection represents the outward current flowing from the *trans* to *cis* side. (B). The single-channel current-voltage relationship in the various Cs⁺ concentrations. (C). The Cs⁺-concentration dependency of the single-channel current amplitude at different membrane potentials. (D). The Eadie-Hofstee plot. The concentration dependent unitary currents were plotted as a function of the single channel current. From the fitted lines, the dissociation constants are obtained: 0.43 M, 0.85 M and 1.43 M at +200 mV, at +300 mV and at +400 mV, respectively.

similar to those for Cs⁺ permeation. The mobility of Cs⁺ and K⁺ in the aqueous solution differs only slightly. Thus, the single-channel conductance of Cs⁺ more than twice than that of K⁺ suggests that the rate-determining step for ion permeation is in the pore.

The apparent saturation of the permeation of Cs⁺ through the pTB channel is characterized by a linear transformation of an Eadie-Hofstee plot (Fig. 2D), in which the horizontal axis represents the single channel current (*i*)/*C* (concentration) and the vertical axis represents the *i*². The data points were fitted with a linear function. The binding constants (*K_d*) were 0.43 M, 0.85 M and 1.43 M for 200 mV, 300 mV and 400 mV, respectively. The linear fit suggests that, unlike the gA channel, the β -helical pore formed by the pTB molecule holds only one ion at a time (i.e. the one-ion pore¹⁵), even for the most permeable Cs⁺. For more persuasive experimental evidence, the mole-fraction experiment was then performed.

The mole-fraction behavior of the *V_{rev}* in the mixed solutions. The mole-fraction experiment is the method of choice for elucidating whether the pore has the capacity to bear multiple ions of different species at the same time. Here the mole-fraction behavior of the *V_{rev}* using different ionic compositions was examined. In the event that the *V_{rev}* did not monotonically change, but rather exhibited a typical maximum value in the course of the progressive changes in the molar ratio, then we called this “anomalous mole-fraction behavior” i.e. the behavior originating from the interactions between the permeating ions within the pore (multi-ion pore^{15,21,22}).



The experimental configuration is depicted in Fig. 3A. The *trans* compartment was bathed with the 3 M CsCl solution throughout the experiment, while the *cis* compartment was varied in terms of the composition (i.e. the mole-fraction) of the permeating ions (Cs^+ and K^+), while maintaining the total concentration of these ion species at 3 M. The V_{rev} shifted nearly linearly along with the decreases in the Cs^+ mole-fraction in the *cis* compartment (Fig. 3B, blue symbols). The value reached -14 mV in the bi-ionic condition (i.e. single ion species on either side of the membrane), a condition in which we previously determined the permeability ratio of the Cs^+ against K^+ ($P_{\text{Cs}}/P_{\text{K}}$) to be 1.7¹. The permeability ratio is defined based on the Goldman-Hodgkin-Katz (GHK) equation, and here the shift of the V_{rev} in the mole fraction was fitted by the GHK equation. In accordance with the experimental data, the GHK function (Fig. 3B, the dotted line) is curved slight. Thus, it can be inferred that the permeating ion species do not interact each other upon permeation^{20,21}.

Similar mole-fraction experiments were performed for the total concentration of 1.0 M, and the nearly linear relationship was obtained (Supplement Fig. S1C).

Anomalous mole fraction behavior is most typically seen when two ion species show similar conductance. For the pTB channel, the single-channel conductance of Cs^+ and Rb^+ is 18 pS and 12 pS, respectively at 3 M¹. The mole fraction experiment for Cs^+ and Rb^+ revealed that the V_{rev} nearly linearly shifted as the mole fraction of Cs^+ was changed (Fig. 3B, green symbols).

These results strongly suggest that the pTB channel is one-ion channel.

The concentration dependency of the V_{rev} in the bi-ionic conditions. Constant V_{rev} values at a fixed ratio of two ion species but with different concentrations are another clue supporting the one-ion pore. The V_{rev} in the bi-ionic condition was measured at different concentrations of the pure Cs^+ (*trans* compartment) and K^+ (*cis* compartment) solutions. The V_{rev} did not change significantly from 0.1 M to 3 M (Fig. 3C), further supporting the one-ion pore.

In the above analyses, the GHK equation has been used. However, the equation is formulated with an assumed independence of ions permeating through the membrane phase under a constant electric field across the membrane²², and the detailed pore structure cannot be taken into consideration. To further interpret the mole-fraction data and the underlying process of permeation and selectivity through the pore, we performed model analysis.

An ion permeation model of the pTB channel in the case of the pure solutions. To characterize the permeation properties of the pTB channel, the permeation kinetics were expressed with a discrete-state Markov model (DSMM^{24–26}), rather than a continuum model of the Poisson-Nernst-Planck theory^{31–35}. This is because of the simplicity of the experimental data analysis³⁶. Based on the structural similarity, the permeation model used for the gA channel was also employed for the pTB channel (i.e. the two-site three-barrier model: There are two binding sites at both ends of the channel; see Fig. 6A). In contrast to the gA channel, which has the symmetric structure of a head-to-head dimer, the pTB channel is formed by a single molecule, and the weakly rectified *i-V* curves suggest that the potential profile is asymmetric.

For the purpose of model fitting, the double-occupancy state was initially excluded from the model because of saturation (i.e. the three-state [3-state] model; Fig. 4A). The voltage-dependent rate constants (the five free parameters) in the 3-state model were optimized for the experimental data, including the voltage- and concentration-dependent single-channel current amplitudes. As shown in Fig. 2 (the broken lines), the data were well fit using the 3-state model (see the supplement for the rate constants).

For the sake of completeness, additional fitting was performed using the four-state model involving the double-occupancy state (Fig. 6A). However, the goodness of the fit was not substantially

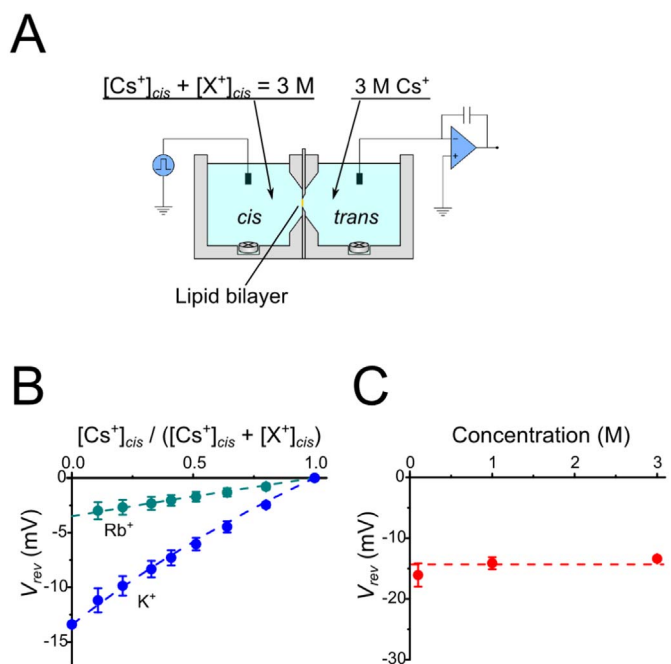


Figure 3 | The mole-fraction behavior of the V_{rev} of the pTB channel. (A). The experimental configuration of the ionic solutions in the two compartments of the chamber. pTB was added to the *cis* compartment. The *trans* compartment was kept constant at 3 M Cs^+ . The mole fraction of the Cs^+ and X^+ concentrations was changed in the *cis* compartment, while the sum of the concentrations were fixed so as to be constant at 3 M. (B). The mole-fraction behavior of the V_{rev} in Cs^+ vs. K^+ and Cs^+ vs. Rb^+ solutions. The shift of the V_{rev} was plotted for the mole fraction of Cs^+ in the *cis* compartment. The dotted lines are the curve deduced from the Goldman-Hodgkin-Katz (GHK) equation. (C). The V_{rev} in the bi-ionic condition in pure Cs^+ (*trans*) and pure K^+ (*cis*) solutions under different concentrations.

improved by increasing the number of the free parameters from 5 for the 3-state model to 8 for the 4-state model. We also examined the simplest 2-state model, and it turned out to be inadequate for the voltage- and concentration-dependency data. Thus, we conclude that the 3-state model is adequate for accounting for the experimental data on Cs^+ permeation.

A similar model analysis was performed in parallel, and the rate constants for the K^+ permeation in the 3-state model were optimized using the data shown in the supplement (Fig. S1). These results indicate that there are two ion binding sites along the pore, but ions of the same species never occupy these sites simultaneously.

Cs^+ vs. K^+ permeation. To compare the differences in the permeation of Cs^+ and K^+ , the rate constants were expressed in a profile such that the height represents the logarithm of the rate constants, and the horizontal axis the voltage dependency index for each rate constant (or the electrical distance) (Fig. 4B). The profile itself does not have actual physical significance, but the superimposed profiles provide a visualization of the contrast between the rate constants of the two ion species.

The profiles are slightly asymmetric for both Cs^+ and K^+ permeation. There are two troughs near both ends in terms of the electrical distance, originating from electrostatic factors^{9,37}, which is in accord with the findings for the gA channel. The permeating ions readily occupy either of these sites, and the binding to the extracellular (the right side) site is slightly more stable than the intracellular (the left side) site. The predominant barrier is against the transfer of an ion across the pore (the central barrier). The slight differences in the

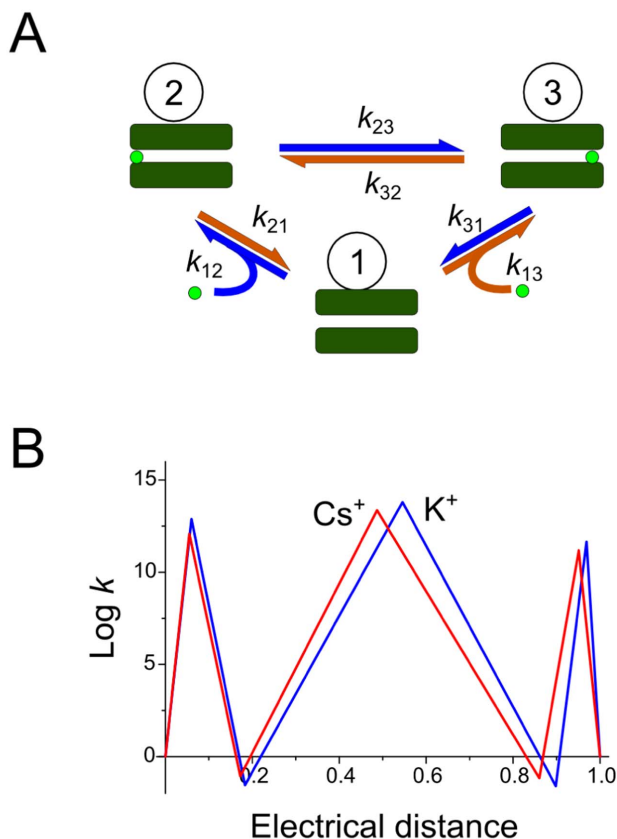


Figure 4 | The permeation model of the pTB channel. (A). The three-state model. The permeation proceeds by the following steps. An ion approaches the empty pore and binds inside the pore near the entrance. In the pore, the ion moves from one site to another, and then exits. These permeation processes are expressed with three discrete states and the transitions between them. Among the rate constants, there are included the second-order rate constants (k_{12} and k_{13}) in the process of ion association from the bulk solution. For instance, k_{12} is the rate constant representing the ion binding from the left-side (the intracellular side). (B). A profile deduced from the rate constants for the Cs^+ and K^+ permeation at 1 M. The set of rate constants was converted to a profile in which the vertical axis represents the logarithm of the rate constants and the horizontal axis indicates the electrical distance.

shape of the profiles for these ion species mostly reside in the depth of the two binding sites.

Ion permeation model for the pTB channel in the case of mixed solutions. The above model characterizes the permeation for the pure solutions, but we wanted to understand the underlying events of the non-anomalous behavior that determined whether two ion species might interact in the pore. From the previous model fitting results, the two sets of model parameters for the Cs^+ and K^+ permeation process allowed us to build a permeation model for the mixed ion solutions. Combining the two 3-state models for Cs^+ and K^+ generates a five-state model that shares the empty state for both Cs^+ and K^+ permeation processes (Fig. 6C).

The rate constants for Cs^+ and K^+ permeation that were determined separately in the pure solutions reproduce the shift that occurred in the V_{rev} in the mixed solution qualitatively, but not quantitatively. Thus, the rate constants for K^+ permeation were further optimized such that the shift in the V_{rev} as well as the i - V and i - C curves was reproduced.

The solid line superimposed on Fig. 5 indicates the calculated values, and thus the mutual exclusion model without any double-occupancy states (5-state model) successfully accounts for all the

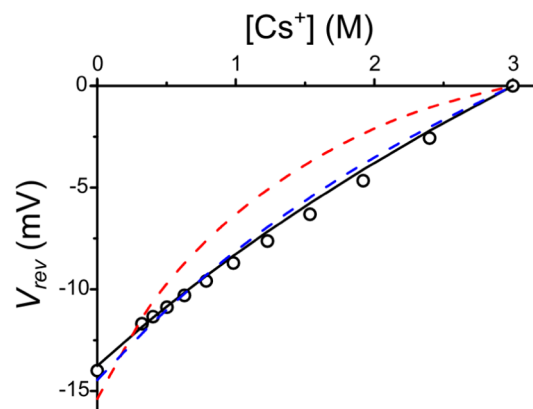


Figure 5 | Simulated mole fraction behavior for the different binding modes in the channel permeation model. The solid line indicates the mole fraction behavior for the 5-state model and the curved, broken line indicates the 7-state model for the independent binding of the two ion species at both ends (red) and the hundred times less affinity to the second ion binding (blue).

experimental data. In the pTB channel, an ion cannot gain access to the pore once another ion of a different species has already occupied it.

Anomalous mole fraction data. In the mole-fraction relationship for the V_{rev} shift, we found that the 5-state model gave slightly curved, rather than straight linear. This means that the apparent “anomalousness” must be related to the degree of the curvature. Here we include two additional states for the possible occurrence of two ion species simultaneously taking part in the permeation process (the 7-state model; Fig. 6D), and the anomalousness and the degree of curvature can be related.

In the 7-state model, eight rate constants (six free parameters: k_{36} , k_{64} , k_{46} , k_{57} , k_{72} and k_{27}) for the transitions towards and away from the mixed ion-species occupied states (states 6 and 7 in model C shown in Fig. 6) must be determined. One can postulate a permeation event involving double occupancy states such that an ion binds to the pore whether the other site is already occupied or not. In this double-occupancy model, the rate constants for the first and second binding events are identical (e.g., $k_{12} = k_{57}$ etc.). The mole fraction behavior is shown as the highly curved red broken line in Fig. 5.

On the 7-state model, the one-ion pore feature can be attained by setting the affinity for the second ion binding extremely low, being equivalent to the 5-state model. To set the model parameters for an intermediate situation, the second ion was assumed to bind with the hundred times less affinity than the first ion. The curve slightly deviated from the experimental data (Fig. 5, blue broken line). Thus, the mole fraction data supports practically the one-ion pore.

Discussion

In the present study we have examined the permeation features of the pTB channel by focusing on the one-ion characteristics of the channel by means of a step-by-step, more comprehensive approach. Starting from the simple saturation of the concentration dependent single-channel current, the V_{rev} was measured in both the mole fraction conditions and bi-ionic conditions at different concentrations, and then the model analyses were performed. To characterize the experimental results, we applied the discrete-state Markov model exclusively, although more elaborated modeling with the Poisson-Nernst-Planck equation has been applied recently for other channels^{31–35}.

All the processes used in the model fitting and model discrimination in the present study are summarized in Fig. 6. In the case of the pure solution, the doubly-occupied states for the same ion species

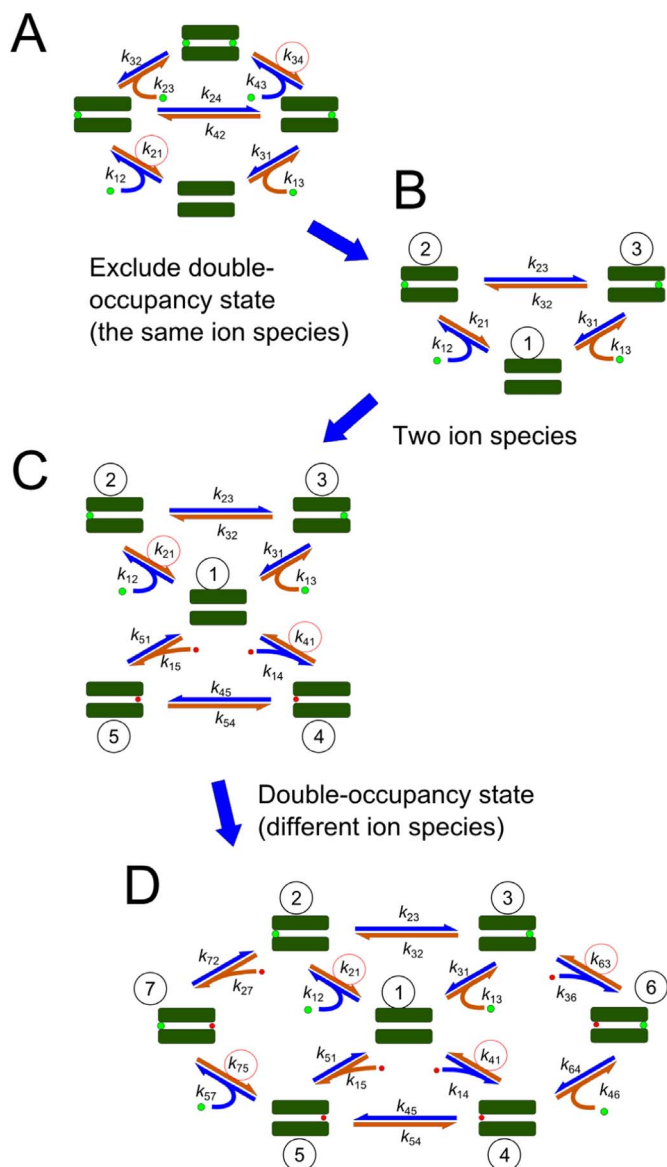


Figure 6 | The optimal model for permeation through the pTB channel in the pure and mixed solutions. Starting from the four-state model analogous to that used for the gA channel (A), the models accounting for the experimental data were selected. In model (A), the double-occupancy state was eliminated based on the saturation behavior of the ion conduction, and model (B) is adequate for the pure solutions of Cs^+ and K^+ . In the mixed solution, two three-state models were integrated into a five-state model (C). For completeness of the analysis, two double-occupancy states were included for possible interaction between the two ion species in the pore, leading to the seven-state model (D). The nearly linear mole fraction data indicated that model (C) is well matched to the mixed solution of Cs^+ , K^+ and Rb^+ .

were not involved, and the 3-state model was thus deemed more appropriate. On the other hand, the two-state model was insufficient to reproduce the data. For the mixed solutions, the 3-state model was extended to the 5-state model, which reproduced all the experimental data.

From all the aspects examined, it is concluded that although there are two ion binding sites in the pTB channel, these sites are never occupied by two ions simultaneously, neither by the same ion species nor by the different ion species of Cs^+ and K^+ .

Notwithstanding the fact that it possesses a similar β -helical structure, the pTB channel exhibited different permeation features than

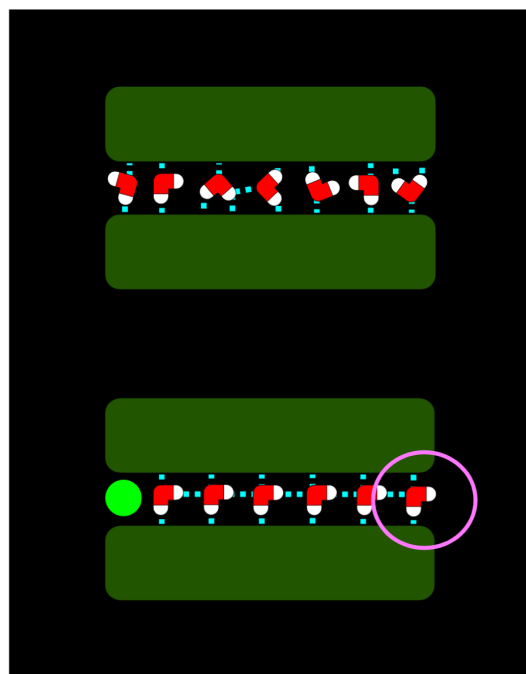


Figure 7 | A hypothetical model of the one-ion pore. In the narrow pore, ions and water are aligned in a single-file column (The number of water molecules in the pTB channel is not known, and the figure shows an arbitrary number.). In the event that an ion locates at the end of the pore, the water molecules in the pore are likely to be oriented with their dipolar vectors pointing away from the ion, forming hydrogen bonds both with each other and with the backbone. The realignment of the water molecules towards the bound ion in the pore should be rapid enough that it is completed before the second ion approaches the pore from the opposite end. When a second ion approaches the opposite binding site from the bulk solution, the water molecule at the end must be turned for the purpose of solvating the incoming ion, or the end water molecule would escape from the pore by an exchange of the ion. Here we hypothesize that the water molecule at the end of the pore is tightly oriented (magenta circle), and thus the incoming ion cannot replace the water already at the site.

the gA channel with respect to the one-ion pore. Why is it that a pore as long as 45 Å cannot hold multiple ions? Given the two binding sites at both ends in both the pTB and gA channels, the one-ion permeation process requires a rational account for why the second ion is excluded. In case of the gA channel, Na^+ is exceptional such that it permeates through the gA channel with one-ion characteristics¹¹, while the mechanism underlying the ion-ion pore still remains elusive³⁸. A signal of some sort of ion binding at one end of the pore must be conveyed towards the opposite end to stop another ion from entering. If the binding sites are close to each other, the electrostatic repulsion between the ions displaces the second ion and thus does not allow simultaneous double occupancy. In this electrostatic context, the double Cs^+ occupancy in the short gA channel and the single Cs^+ occupancy in the long pTB channel are obviously paradoxical.

We propose here two competing hypotheses for the second ion exclusion. First, the hydrogen bond network in the peptide backbone may play a role. When a first ion enters into the pore after partial dehydration, it is coordinated by the backbone carbonyls. It has been shown that the carbonyls slightly change their orientation such that the carbonyl oxygen approaches the bare ion. This movement is called “carbonyl libration”^{39,40}. To prevent the second ion from entering, the local backbone structure that is engaged in coordinating a bound ion propagates a structural change throughout the molecule such that the entrance barrier increases substantially. This cooperative structural change may occur in pTB, but it is questionable



Table 1 | Molecular properties of polytheonamide B and gramicidin A

	Polytheonamide B	Gramicidin A
Origin	Symbiotic bacteria	Bacteria <i>Bacillus brevis</i>
Chemical features		
Number of amino acid residues	48	15
Molecular weight (Da)	5032	1882.3
Amino acid chiral	L- and D-	←
Unusual amino acid side chain	Many (Msn, ...)	none
Structure of ion channel	$\beta^{6:3}$ helix	←
PDB code	2RQO	1TKQ
Inner pore diameter	4 Å	←
Helix length	45 Å in the organic solvent	26 Å in the membrane
Side-chain hydrogen bonds	+	-
Stoichiometry of channel formation	monomer	head-to-head dimer
Conductance (at 300 mV in 2 M CsCl)	20 pS	56 pS
Ion selectivity	Monovalent cations	←
Selectivity sequence ^c	H ⁺ > Cs ⁺ > Rb ⁺ , K ⁺ , Na ⁺ , Li ⁺	←
Gating	Conformational change?	Spontaneous dimer formation
Efficient membrane insertion	Added in one side	Added in both sides
Maximum number of ions in the channel	1	2
Cytotoxicity: IC ₅₀ (nM) ^a	< 0.2	4.3 ^b

^aValues determined against P388 mouse leukemia cells.

^bCytotoxicity of gramicidin D (mixture of gramicidin A, B and C with a ratio of 1 : 0.075 : 0.175).

^cBoth the permeability ratio and the single channel conductance give the same sequence.

whether such a cooperative structural change would be fast enough to exclude rapidly accessing second ion.

Alternatively, a contribution by the water molecules in the pore may occur. The water molecules in the pore are aligned along the pore for solvating the occupying ion such that the oxygen is pointing towards the bound ion (i.e. the single-file water molecule column). They form hydrogen bonds with each other and with the backbone amides and carbonyls^{41–43} (Fig. 7). In the gA channel, the molecular dynamics simulation revealed that the water molecules in the pore are strongly attracted toward the singly occupying ion due to the long range electrostatic interactions which take place with the single-file becoming slightly compressed^{38,42}, although the dimer junction at the center may disturb the continuity. The relaxation time for generating this columnar configuration was rapid. If this configuration of water molecules with long-range coupling of the water column is more stable in the pTB channel than in the gA channel, then the water molecule at the opposite end would generate an unfavorable entrance barrier for an incoming ion before it had time to gain access. The single file configuration of the water molecules imposed by the long, narrow pore of the pTB channel may lead to a closer contact with the nearest water molecule, and this unusual allocation of pore space is in its own right an intriguing issue for further studies in the context of the one-ion pore hypothesis.

The molecular features of the pTB channel compared with the gA channel are summarized in Table 1. Their contrasting features are expected to be related to the different cytotoxic activity of the two peptides. Further characterization of the pTB channel is currently underway in our laboratory.

Methods

Single-channel current recordings. Single-channel currents were measured using the planar lipid bilayer method at room temperature¹. A Teflon sheet of 0.5 mm thickness was used as a partition dividing two compartments, on which a hole (< 100 μm diameter) was made. The membrane was formed from diphytanoylphosphatidylcholine (Avanti Polar Lipids, Alabaster, AL, USA) dissolved in *n*-decane (Nacalai, Kyoto, Japan) at a concentration of 20 mg/ml. The *cis* and *trans* compartments were filled with ionic solution containing CsCl or KCl (Nacalai, Kyoto, Japan). The reference electrode was placed in the *cis* compartment, to which polytheonamide B (pTB) was added at a final concentration of 100 fM. The membrane potential was defined as the *trans* side relative to the *cis* side, and the current flowing from the *trans* side to the *cis* side as outward, indicated by a “+” sign, mimicking a target cell membrane accessed by pTB from the *cis* (extracellular) side (Fig. 3A). The current data were recorded and stored on a PC using pCLAMP

software (Molecular Devices, Sunnyvale, CA, USA) through an Axopatch 200B amplifier and Digidata 1322A digitizer (Molecular Devices, Sunnyvale, CA, USA). The low pass filter was set at 2 kHz for the cut-off frequency, and the data were sampled at 10 kHz.

Analysis of the mole-fraction behavior. The mole-fraction behavior of the bi-ionic potential was evaluated as follows. The *trans* compartment was filled with 3 M CsCl and kept constant throughout the experiment. The mole fraction of CsCl and KCl in the *cis* compartment was changed, while the sum of the concentrations was fixed at 3 M (Fig. 3B). pTB was added to the *cis* compartment at a final concentration of 1 nM. The V_{rev} of the macroscopic current of pTB was obtained by applying the voltage-ramp command to the membrane (x mV/s). V_{rev} was plotted against the mole fraction of Cs⁺ in the *cis* compartment. Similar experiments were performed for the Cs⁺ and Rb⁺ at 3 M (Fig. 3B), and Cs⁺ and K⁺ at 1 M (Supplement Fig. S1C).

The mole fraction data were fitted with the Goldman-Hodgkin-Katz (GHK) equation,

$$V_{rev} = -\frac{RT}{F} \ln \frac{P_{Cs}}{(P_{Cs} - P_X) \cdot \left(\frac{[Cs^+]_{cis}}{[Cs^+]_{cis} + [X^+]_{cis}} \right) + P_X}$$

where R is the gas constant; T , the absolute temperature; F , Faraday's constant; P_X , the permeability of X ; $[X]_{cis}$, the concentration of X in the *cis* compartment.

Permeation model. The single-channel current data were used to construct the permeation model. The ion permeation process has already been established for the gA channel, in which a two binding sites-three barrier (4-state) model characterizes the various aspects of the permeation properties²⁴. From the analogous pore structure of the pTB channel, the 4-state model was employed as the initial model. In contrast to the gA channel formed by the head-to-head dimer, the pTB channel is formed by monomer, and the potential profile for the permeation of the pTB channel is asymmetric in shape. Accordingly, additional parameters are necessary for characterizing the pTB channel compared to the gA channel. For instance, the rate constants, such as those for an ion gaining access to the pore from the *cis* side or *trans* side, were set differently. The voltage-dependent rate constant for the transition from the i to j state (the first-order rate constant) is defined such that

$$k_{ij} = k_{ij}^0 \exp[-deV/kT]$$

where k_{ij}^0 is the rate constant at 0 mV, d the electrical distance, e the elementary charge, k the Boltzman constant and T the absolute temperature. Similarly, the concentration-dependent (the second-order) rate constants are defined as,

$$k_{ij} = c k_{ij}^c \exp[-deV/kT]$$

where c represents the concentration in M. The net flux was calculated from the steady-state probability of the states and the rate constants.

Mixed solution model. To characterize the bi-ionic potential and the shift of the V_{rev} in the mole fraction experiment, we extended the model to two ion species in mixed solution. Including the possible contribution of the doubly-occupied states of two



different ion species, the model is described with seven states (see Fig. 6D). The net flux was calculated from the conventional matrix method²⁶.

The rate constant matrix is shown in the supplement.

Rate-constant optimization. The sum of the χ square values between the data values and the calculated values were optimized.

All of the model calculations were performed using Mathematica (Wolfram Research, Inc. Champaign, IL, USA).

- Iwamoto, M., Shimizu, H., Muramatsu, I. & Oiki, S. A cytotoxic peptide from a marine sponge exhibits ion channel activity through vectorial-insertion into the membrane. *FEBS Lett.* **584**, 3995–3999 (2010).
- Hamada, T., Sugawara, T., Matsunaga, S. & Fusetani, N. Polytheonamides, unprecedented highly cytotoxic polypeptides, from the marine sponge theonella swinhoei. *Tetrahedron Lett.* **35**, 719–720 (1994).
- Oiki, S., Muramatsu, I., Matsunaga, S. & Fusetani, N. A channel-forming peptide toxin: polytheonamide from marine sponge (*Theonella swinhoei*). *Nihon Yakurigaku Zasshi.* **110 Suppl.**, 195P–198P (1997).
- Hamada, T., Matsunaga, S., Yano, G. & Fusetani, N. Polytheonamides A and B, highly cytotoxic, linear polypeptides with unprecedented structural features, from the marine sponge, *Theonella swinhoei*. *J. Am. Chem. Soc.* **127**, 110–8 (2005).
- Inoue, M. *et al.* Total synthesis of the large non-ribosomal peptide polytheonamide B. *Nat. Chem.* **2**, 280–5 (2010).
- Freeman, M. F. *et al.* Metagenome mining reveals polytheonamides as posttranslationally modified ribosomal peptides. *Science* **338**, 387–90 (2012).
- Ducho, C. Convergence leads to success: total synthesis of the complex nonribosomal peptide polytheonamide B. *Angew. Chem. Int. Ed. Engl.* **49**, 5034–6 (2010).
- Hamada, T. *et al.* Solution structure of polytheonamide B, a highly cytotoxic nonribosomal polypeptide from marine sponge. *J. Am. Chem. Soc.* **132**, 12941–5 (2010).
- Andersen, O. S. Gramicidin channels. *Annu. Rev. Physiol.* **46**, 531–48 (1984).
- Shinohara, N., Itoh, H., Matsuoka, S. & Inoue, M. Selective modification of the N-terminal structure of polytheonamide B significantly changes its cytotoxicity and activity as an ion channel. *ChemMedChem* **7**, 1770–3 (2012).
- Finkelstein, A. & Andersen, O. S. The gramicidin channel: A review of its permeability characteristics with special reference to the single-file aspect of transport. *J. Membr. Biol.* **59**, 155–171 (1981).
- Valiyaveetil, F. I., Sekedat, M., Mackinnon, R. & Muir, T. W. Glycine as a D-amino acid surrogate in the K⁺-selectivity filter. *Proc. Natl. Acad. Sci. U. S. A.* **101**, 17045–17049 (2004).
- Valiyaveetil, F. I., Leonetti, M., Muir, T. W. & Mackinnon, R. Ion selectivity in a semisynthetic K⁺ channel locked in the conductive conformation. *Science* **314**, 1004–1007 (2006).
- Valiyaveetil, F. I., MacKinnon, R. & Muir, T. W. Semisynthesis and folding of the potassium channel KcsA. *J. Am. Chem. Soc.* **124**, 9113–9120 (2002).
- Hille, B. Potassium channels as multi-ion single-file pores. *J. Gen. Physiol.* **72**, 409–442 (1978).
- Hodgkin, A. L. & Keynes, R. D. The potassium permeability of a giant nerve fibre. *J. Physiol.* **128**, 61–88 (1955).
- Ketchum, R. R., Hu, W. & Cross, T. A. High-resolution conformation of gramicidin A in a lipid bilayer by solid-state NMR. *Science* **261**, 1457–60 (1993).
- Urban, B. W., Hladky, S. B. & Haydon, D. A. Ion movements in gramicidin pores. An example of single-file transport. *Biochim. Biophys. Acta - Biomembr.* **602**, 331–354 (1980).
- Hladky, S. B. & Haydon, D. A. Ion transfer across lipid membranes in the presence of gramicidin A. *Biochim. Biophys. Acta - Biomembr.* **274**, 294–312 (1972).
- Eisenman, G., Latorre, R. & Miller, C. Multi-ion conduction and selectivity in the high-conductance Ca⁺⁺-activated K⁺ channel from skeletal muscle. *Biophys. J.* **50**, 1025–1034 (1986).
- Hagiwara, S., Miyazaki, S., Krasne, S. & Ciani, S. Anomalous permeabilities of the egg cell membrane of a starfish in K⁺-TI⁺ mixtures. *J. Gen. Physiol.* **70**, 269–81 (1977).
- Hille, B. *Ionic Channels of Excitable Membranes*. Sinauer Associates (2001).
- Hladky, S. B. & Haydon, D. A. Ion movements in gramicidin channels. *Curr. Top. Membr. Transp.* **21**, 327–372 (1984).
- Andersen, O. S. Kinetics of ion movement mediated by carriers and channels. *Methods Enzymol.* **171**, 62–112 (1989).
- Oiki, S., Iwamoto, M. & Sumikama, T. A mesoscopic approach to understanding the mechanisms underlying the ion permeation on the discrete-state diagram. *J. Gen. Physiol.* **136**, 363–365 (2010).
- Oiki, S., Iwamoto, M. & Sumikama, T. Cycle flux algebra for ion and water flux through the KcsA channel single-file pore links microscopic trajectories and macroscopic observables. *PLoS One* **6**, e16578 (2011).
- Urban, B. W., Hladky, S. B. & Haydon, D. A. The kinetics of ion movements in the gramicidin channel. *Fed. Proc.* **37**, 2628–32 (1978).
- Oiki, S., Koeppe, R. E. & Andersen, O. S. Voltage-dependent gating of an asymmetric gramicidin channel. *Proc. Natl. Acad. Sci. U. S. A.* **92**, 2121–2125 (1995).
- Oiki, S., Koeppe, R. E. & Andersen, O. S. Asymmetric gramicidin channels: heterodimeric channels with a single F6Val1 residue. *Biophys. J.* **66**, 1823–1832 (1994).
- Oiki, S., Koeppe, R. E. & Andersen, O. S. A dipolar amino acid substitution induces voltage-dependent transitions between two stable conductance states in gramicidin channels. *Biophys. J.* **62**, 28–30 (1992).
- Bezrukov, S. M., Berezhkovskii, A. M. & Szabo, A. Diffusion model of solute dynamics in a membrane channel: mapping onto the two-site model and optimizing the flux. *J. Chem. Phys.* **127**, 115101 (2007).
- Cárdenas, A. E., Coalsón, R. D. & Kurnikova, M. G. Three-Dimensional Poisson-Nernst-Planck Theory Studies: Influence of Membrane Electrostatics on Gramicidin A Channel Conductance. *Biophys. J.* **79**, 80–93 (2000).
- Corry, B., Kuyucak, S. & Chung, S.-H. Tests of Continuum Theories as Models of Ion Channels. II. Poisson–Nernst–Planck Theory versus Brownian Dynamics. *Biophys. J.* **78**, 2364–2381 (2000).
- Nonner, W., Chen, D. P. & Eisenberg, B. Anomalous Mole Fraction Effect, Electrostatics, and Binding in Ionic Channels. *Biophys. J.* **74**, 2327–2334 (1998).
- Hornig, T.-L., Lin, T.-C., Liu, C. & Eisenberg, B. PNP equations with steric effects: a model of ion flow through channels. *J. Phys. Chem. B* **116**, 11422–41 (2012).
- Miller, C. Ionic Hopping Defended. *J. Gen. Physiol.* **113**, 783–787 (1999).
- Parsegian, A. Energy of an ion crossing a low dielectric membrane: solutions to four relevant electrostatic problems. *Nature* **221**, 844–6 (1969).
- Li, Y., Andersen, O. S. & Roux, B. Energetics of double-ion occupancy in the gramicidin A channel. *J. Phys. Chem. B* **114**, 13881–8 (2010).
- Urry, D. W., Prasad, K. U. & Trapane, T. L. Location of monovalent cation binding sites in the gramicidin channel. *Proc. Natl. Acad. Sci. U. S. A.* **79**, 390–4 (1982).
- Mori, T., Kokubo, H., Oiki, S. & Okamoto, Y. Dynamic structure of the polytheonamide B channel studied by normal mode analysis. *Mol. Simul.* **37**, 975–985 (2011).
- Mackay, D. H., Berens, P. H., Wilson, K. R. & Hagler, A. T. Structure and dynamics of ion transport through gramicidin A. *Biophys. J.* **46**, 229–248 (1984).
- Roux, B., Prod'homme, B. & Karplus, M. Ion transport in the gramicidin channel: molecular dynamics study of single and double occupancy. *Biophys. J.* **68**, 876–892 (1995).
- Jensen, M. Ø., Jogini, V., Eastwood, M. P. & Shaw, D. E. Atomic-level simulation of current-voltage relationships in single-file ion channels. *J. Gen. Physiol.* **141**, 619–32 (2013).

Acknowledgments

We thank Takashi Sumikama for discussion. We thank Grant-in-Aid for Scientific Research on Innovative Areas 2006 (Molecular Science of Fluctuations toward Biological Functions) (23107713) for funding. M.I. and S.O. thank Grant-in-Aid for Scientific Research (B) (23790245) and (23370067, 21107508, 21657038, 20247016) from JSPS. We thank Pacific Edit for reviewing the manuscript prior to submission.

Author contributions

M.I. and S.O. wrote the manuscript. M.I. and S.O. designed research. M.I. performed experiments. M.I., S.M. and S.O. analyzed data. All authors reviewed the manuscript.

Additional information

Supplementary information accompanies this paper at <http://www.nature.com/scientificreports>

Competing financial interests: The authors declare no competing financial interests.

How to cite this article: Iwamoto, M., Matsunaga, S. & Oiki, S. Paradoxical One-ion Pore Behavior of the Long β -Helical Peptide of Marine Cytotoxic Polytheonamide B. *Sci. Rep.* **4**, 3636; DOI:10.1038/srep03636 (2014).



This work is licensed under a Creative Commons Attribution-NonCommercial-NoDerivs 3.0 Unported license. To view a copy of this license, visit <http://creativecommons.org/licenses/by-nc-nd/3.0>